Reaction of Metal Particles in Gas-Phase Detonation Products

V. Tanguay[1], S. Goroshin[1], A. Higgins[1], A. Yoshinaka[2] and F. Zhang[2]
[1]McGill University, Montreal, Quebec, Canada
[2]DRDC Suffield, Medicine Hat, Alberta, Canada

Corresponding author, V. Tanguay: vincent.tanguay@mail.mcgill.ca

Introduction

It has now become common practice to add reactive metal particles (typically, magnesium, aluminum, etc.) to explosives to enhance blast performance. Metal combustion can be very energetic (as much as 3 or 4 times the energy release of typical explosives). Although the total energy released by the metal combustion is significant and comparable to the total energy released by the explosive itself, the timescale of this energy release (timescale for particle reaction) for typical particle sizes (1 to 100 μm), is most probably too long to contribute directly to the detonation front itself. Instead, the metal particles may react with air or even with the detonation products behind the blast wave. It has been shown that the metal particle reaction can significantly increase the strength of the blast and the total impulse delivered to nearby objects or structures (Frost et al. [1, 2]). However, when and where particles react are questions that remain to be answered. It is difficult to obtain quantitative data from full scale experiments using condensed phase explosives

The present study is an experimental investigation using a gas-phase detonation to simulate the conditions in a high explosive fireball. The objective of the present study is to obtain quantitative data for scaling of the ignition and reaction of metal particles in a high explosive environment. The use of a laboratory-scale apparatus utilizing a gas-phase detonation permits better diagnostic access to the reactive particles than can be achieved in field trials with optically thick high explosive products.

Experimental Apparatus

Detonation Tube

The experimental apparatus, consists of a 6.35 cm inner diameter steel tube, 60 cm long. One end of this tube is closed with a blind flange and equipped with an exploding wire-type igniter. The igniter is powered by an 800 J capacitor bank (charged to 4kV). The tube is instrumented with two PCB pressure transducers for characterization of the detonation process and determination of time zero.

The other end of the tube is sealed by a pneumatically actuated gate valve (see Fig. 1). The detonation tube is first evacuated and then filled to 1 atmosphere with a stoichiometric mixture of hydrogen and oxygen. The mixture is prepared by an in-line mixing technique with choked orifices to maintain the flow rate constant irrespective of the downstream pressure. The mass flow rates of hydrogen and oxygen are measured with two FVL-1600 type mass flow meters (Omega Eng. Inc.). Metering valves that

serve as critical orifices allow precise adjustment of the gas flow rates. The oxygen and hydrogen flows are mixed inside a 150 mL stainless steel cylinder filled with ¼ inch stainless steel balls. The quality of the flow control and mixing were verified by measuring oxygen concentration with a NOVA 370 (Nova Analytical Systems Inc., Hamilton, ON) oxygen analyzer.

Once the detonation tube is filled to one atmosphere, the gate valve is opened (the opening time is less than a second). Upon reaching its fully open position, the gate valve activates a micro switch which triggers the ignition system.

Downstream of the gate valve is an approximately one meter long acrylic tube section, open at the far end. Therefore, ambient air fills this section. A knife blade is mounted inside the acrylic tube approximately 50 mm from the gate valve. A small amount of metal powder (5-10 mg) is placed on this blade before an experiment. This technique was also used by Roberts et al. [3]. The aluminum and magnesium powders used were obtained from Valimet Inc. and Reade Manufacturing Co., respectively. The approximate mean particle sizes are shown in Tables 1 and 2.

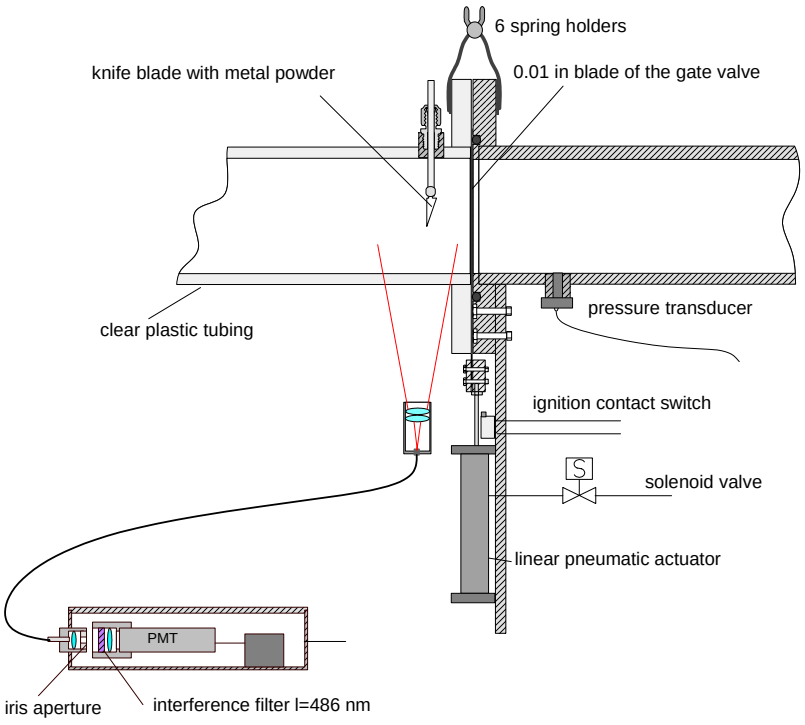

Figure 1. Schematic of experimental apparatus. A pneumatically actuated gate valve separates the steel section (right) from the acrylic section (left).

Table 1. Particle sizes of powders used (aluminum).

Powder	Average Diameter (mean area)
H-2	2.6 μm
H-10	10.2 μm
H-30	32.8 μm
H-50	49.7 μm
H-95	109.3 μm

Table 2. Particle sizes of powders used (magnesium).

Powder	Average Diameter (mean area)
RMC 32.5	44 μm
GRAN 16	60 μm
GRAN 12	85 μm
GRAN 17	240 μm

Photomultiplier

Below the acrylic section of the detonation tube is a short focal distance lens that collects light and transmits it to the photomultiplier assembly (Electron Tubes LTD, UK) by a 1/8 inch fiber optic cable. The light detecting assembly has a frequency bandwidth of 25 MHz and very high sensitivity. A small iris aperture at the front of the photomultiplier is used to attenuate light thus preventing saturation of the amplifier. In the case of aluminum powders, a neutral density filter is also used.

Although the global oxidation of aluminum produces condensed alumina (Al_2O_3), alumina does not exists in the vapor phase. It forms through the processes of chemical condensation (condensation-oxidation) [4] of intermediate gaseous oxides, the most prominent of which is AlO. Thus the appearance of AlO molecular spectra can be used for the detection of Al combustion [3]. The AlO molecular bands are located in a visible range of wavelengths and have a very sharp short-wave boundary.

In the current experiments, a narrow band-pass (10 nm) interference filter with wavelength of approximately 486 nm that coincides with the strongest AlO molecular band is used to detect aluminum combustion.

Results

First, a control experiment was performed with no powder. Figure 2 shows a typical luminosity signal for such a control experiment. A small amount of light can be observed from the detonation products entering the clear section. Several powders were investigated: aluminum (H2, H10, H30, H50 and H95) and magnesium (GRAN 12, GRAN 16, GRAN 17 and RMC 32.5).

Magnesium

Figure 2 shows the comparison between the luminosity emitted by 85 μm magnesium powder and a control experiment without powder. Significant luminosity is observed from the metal powder compared to the control experiment. This luminosity is interpreted as being a result of chemical reaction of the magnesium particle with surrounding gas. It should be noted that aluminum oxide powder was used in a similar experiment. This resulted in no more luminosity than a control experiment without powder. Since aluminum oxide is non-reactive, it can be concluded that the luminosity observed from metal particles is not a result of black body radiation of the hot particles.

Time zero is an estimate of the time at which the transmitted shock reaches the particles on the knife blade. This is not known exactly since the pressure transducers are located

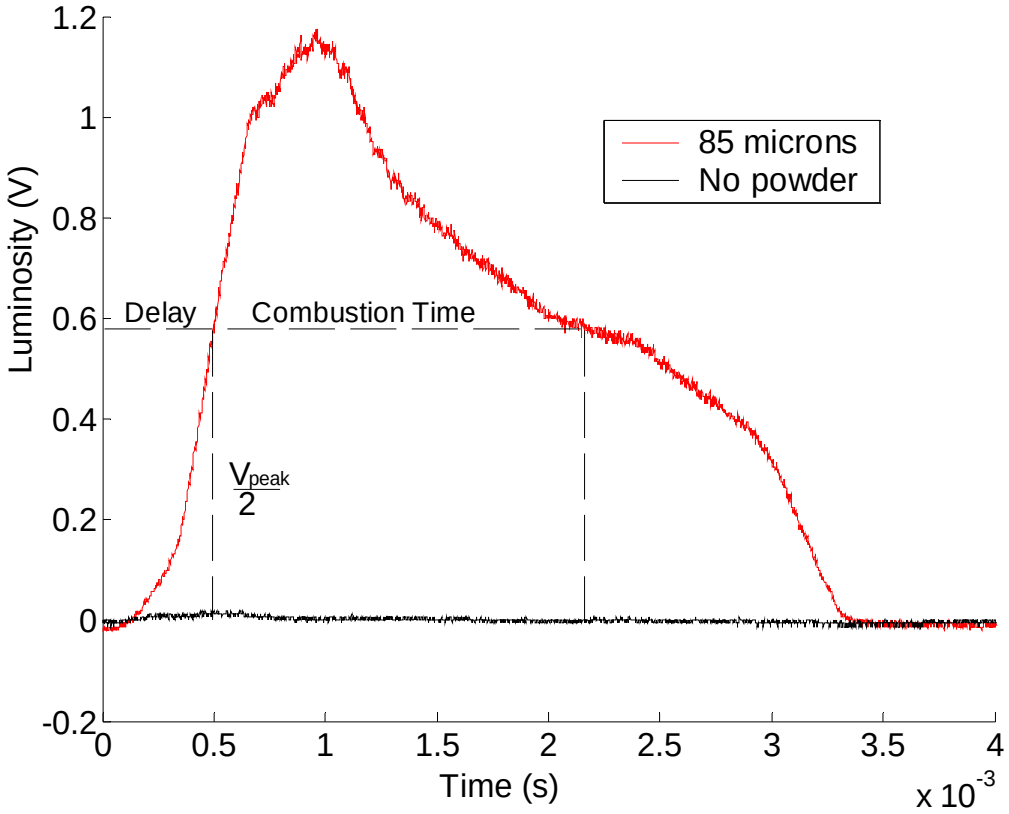

Figure 2. Luminosity emitted by an empty tube (control experiment) and 85 μm magnesium powder. Dashed line construction represents the definitions of delay time and combustion time used in this report.

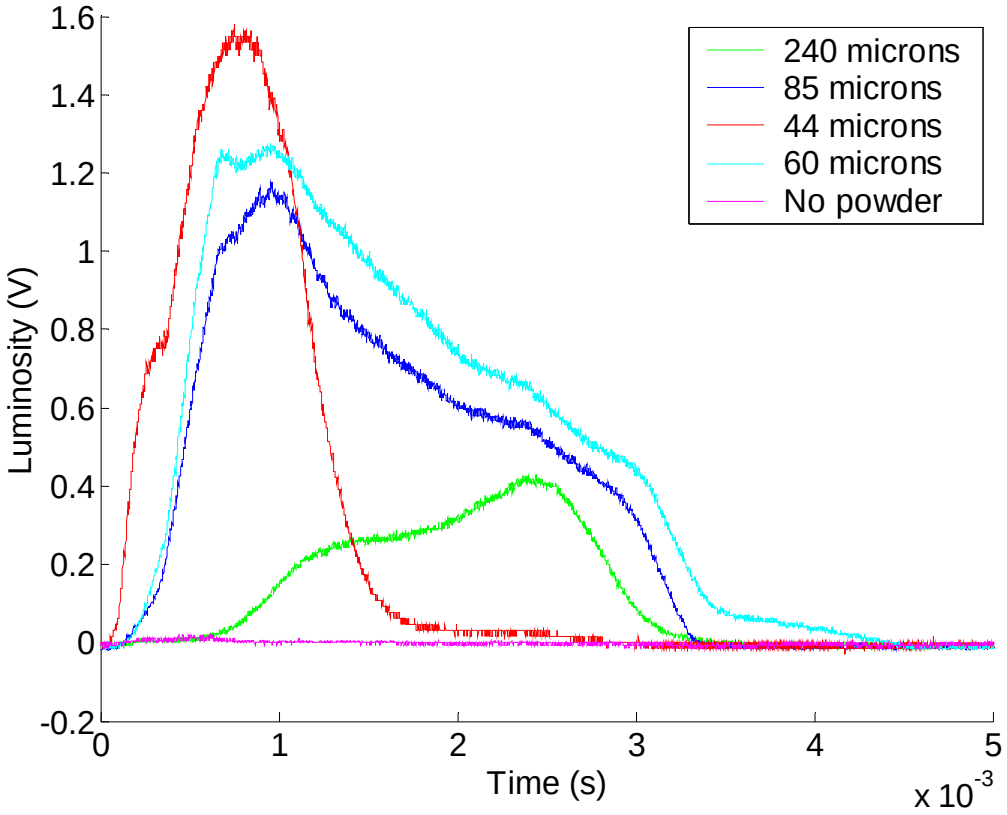

Figure 3. Typical luminosity traces for all the magnesium powders investigated.

inside the steel section. The time it takes for the detonation to go from the second pressure transducer to the gate valve is extrapolated with the detonation velocity obtained from the pressure transducer signals. The time it takes for the transmitted shock to reach the knife is calculated from the transmitted shock strength, which in turn, is calculated with an equilibrium code (NASA's CEA code [5]). This time is on the order of 25-30 μs.

Luminosity is not observed instantaneously from the passage of the transmitted shock wave. However, the delay is quite short (on the order of hundreds of microseconds) depending on the type of metal powder and the particle size. In this study, the delay for luminosity or reaction is defined as the time it takes for the PMT output to reach half the peak amplitude of the signal from the time the transmitted shock reaches the knife. This is the same technique used by Roberts et al. [3] and is illustrated in Fig 2. The duration of reaction, called here reaction time, is defined as the total time during which the luminosity signal exceeds half of its peak value.

For every particle size, several experiments were conducted to ensure reproducibility. Figure 3 shows one typical photomultiplier output for each of the magnesium powders investigated as well as a control experiment without powder. Luminosity is unmistakably

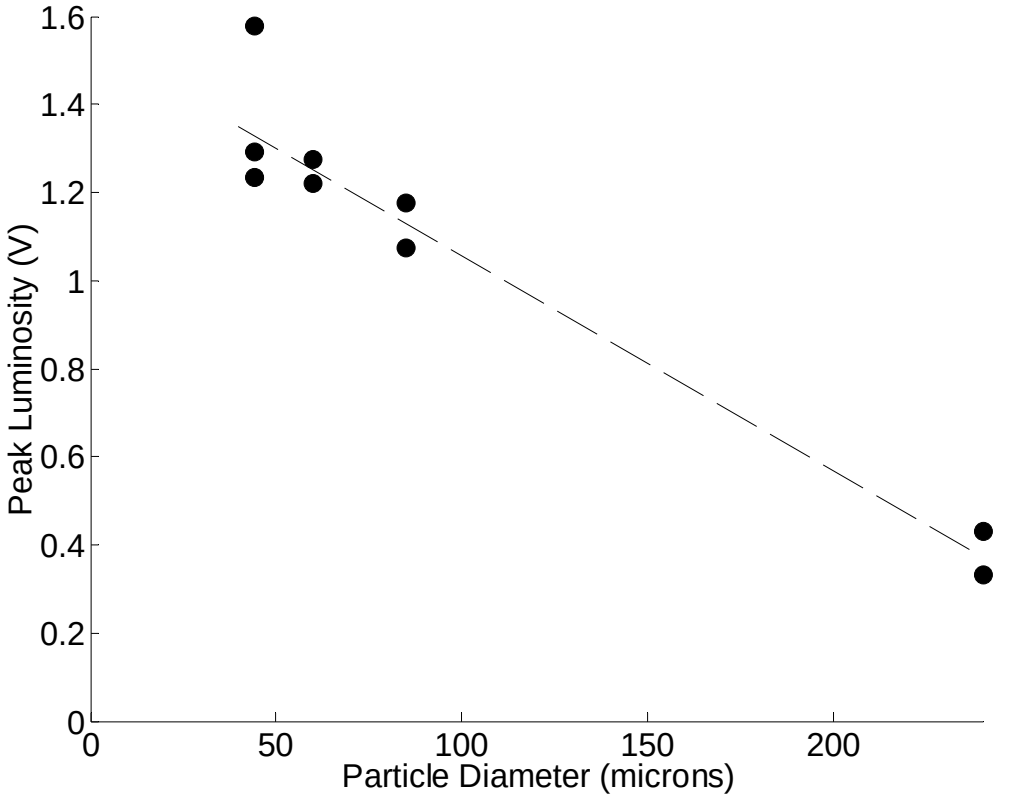

Figure 4. Luminosity amplitude as a function of particle size for all magnesium powders investigated.

emitted by all the magnesium powders meaning all sizes investigated react under the present experimental conditions.

It is apparent from Fig. 3 that the larger particles result in a lower amplitude signal (less luminosity). This is illustrated more explicitly in Fig. 4, which is a plot of the peak amplitude of the PMT output as a function of particle size for all the magnesium powders. This figure clearly shows the decrease of light intensity with increasing particle size. This is presumably explained by the larger specific surface area of the small particles.

Figure 3 also shows that the delay time for chemical reaction increases with increasing particle size. Again, this is shown more clearly in Fig. 5, which shows the delay time versus particle size. Here, the delay is seen to increase with particle size. This is consistent with the view that particles should be heated up to a high enough temperature before chemical reaction occurs. Larger particles certainly take longer to heat up than smaller ones, explaining the longer delay time.

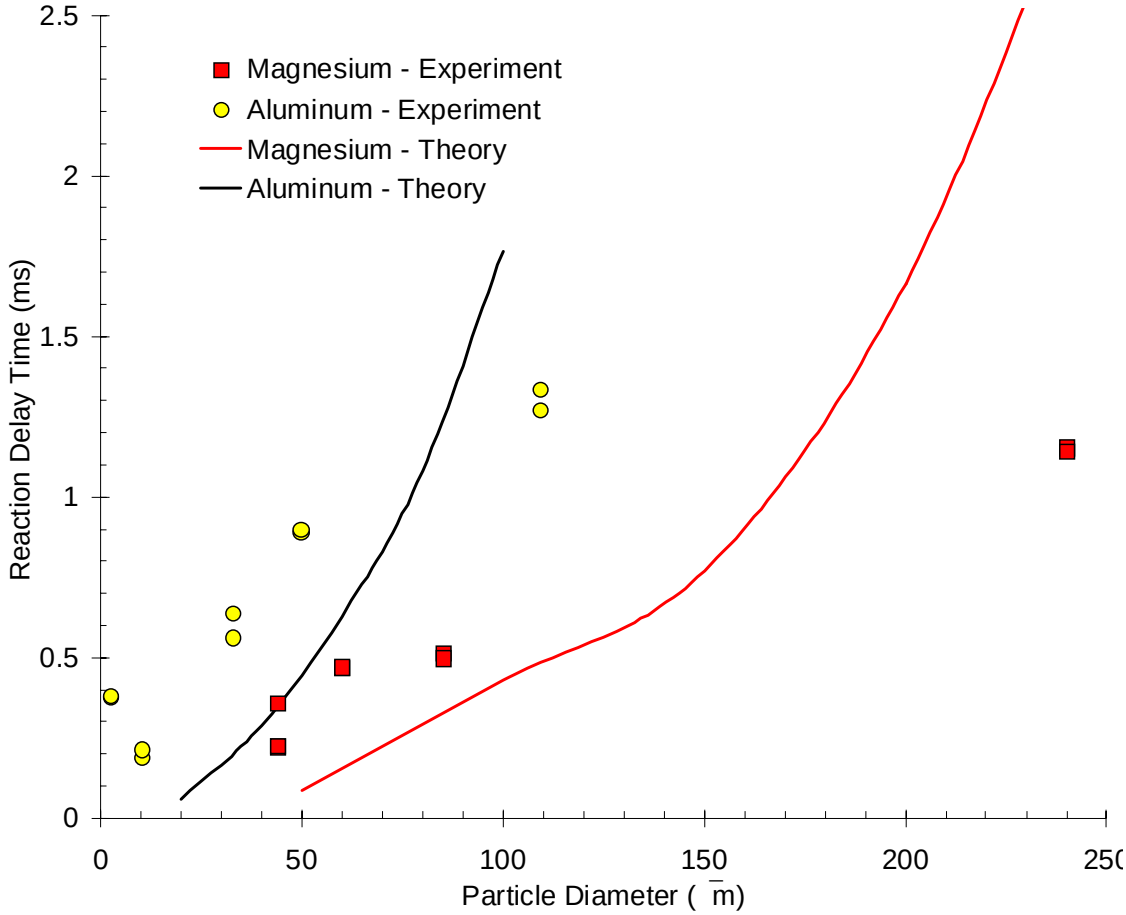

Figure 5. Reaction delay time as a function of particle size for all magnesium and aluminum powders investigated (data point represent experiments and the curves are the result of analytical calculations).

Aluminum

The results for aluminum powders are very similar to the ones for magnesium. Figure 6 shows PMT traces for all the aluminum powders (H2, H10, H30, H50 and H95). Note that contrary to experiments done with magnesium powders, a neutral density filter was used with the photomultiplier. This was done to avoid saturation which was observed with the H2 and H10 powders. As a result, the sensitivity of the photomultiplier was increased to take advantage of the full scale. This higher sensitivity is the cause of the noisier signals on Fig. 6.

For all particle sizes, the amplitude of the luminosity is significantly larger than the control experiments. It should be noted that even though the H95 signal is only slightly larger than the control, this difference can be made unambiguous without the neutral density filter on the PMT (this is not done here as to avoid the smaller particle sizes from saturating the PMT; this way all the aluminum powders can be compared on the same plot).

Figures 5 and 7 show the dependence of the reaction delay time and amplitude, respectively, versus particle size. Qualitatively, the behavior of aluminum is the same as that of magnesium powders: decreasing luminosity and increasing delay time with increasing particle size.

As observed with the magnesium powder, the decrease in luminosity is also quite sharp (almost as sharp as the initial luminosity rise). This leads to a well defined "reaction time" which is plotted versus particle size on Fig. 8. Here, the trend is obvious and the combustion time decreases with increasing particle size.

The fact that the reaction time decreases with particle size is somewhat counterintuitive. One would expect larger particles to burn for a longer time than smaller particles. It may be that the luminosity observed is not related to classical ignition of the particles, i.e. the phenomenon may not be self-sustained combustion. While there is little doubt that the emitted light is a result of chemical reaction, these may not be self-sustained. Perhaps, chemical reaction is occurring only while the conditions of the flow and/or particles meet some sort of minimum or critical conditions for chemical reaction to occur. As soon as the conditions are no longer appropriate to cause chemical reaction, these may stop. Since the detonation tube is quite short, the products may expand and cool sufficiently fast to quench the chemical reactions. If this is the case, one would expect the reaction

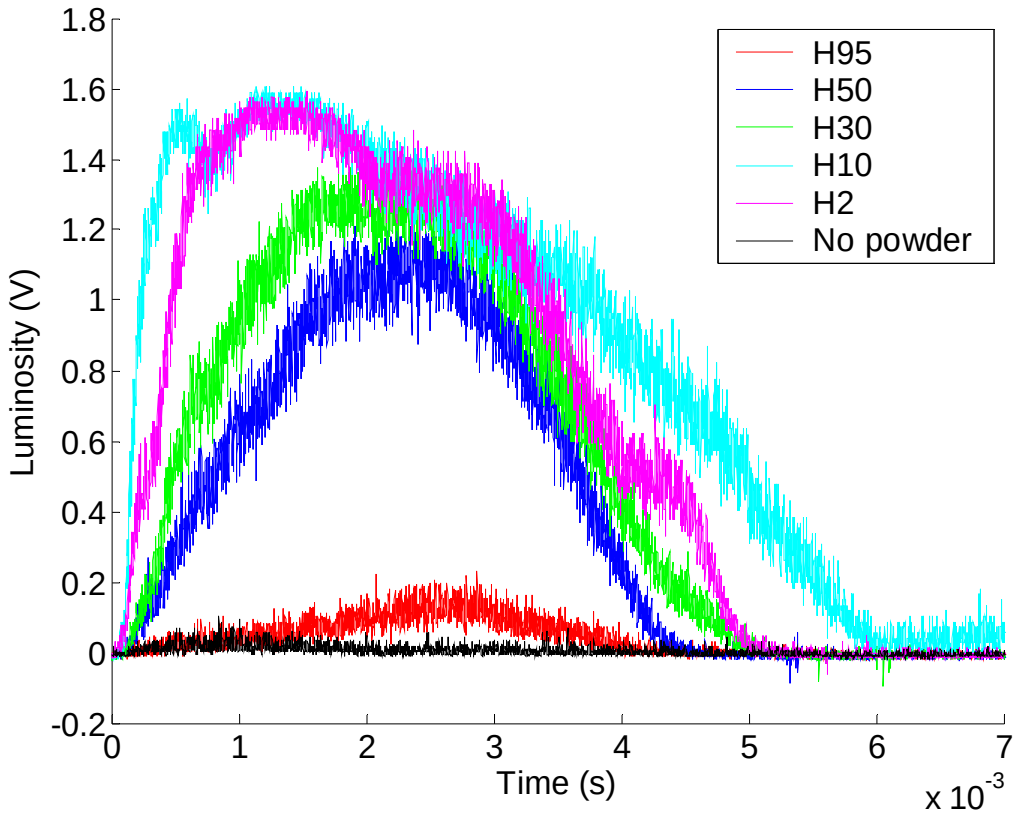

Figure 6. Typical luminosity traces for all the aluminum powders investigated.

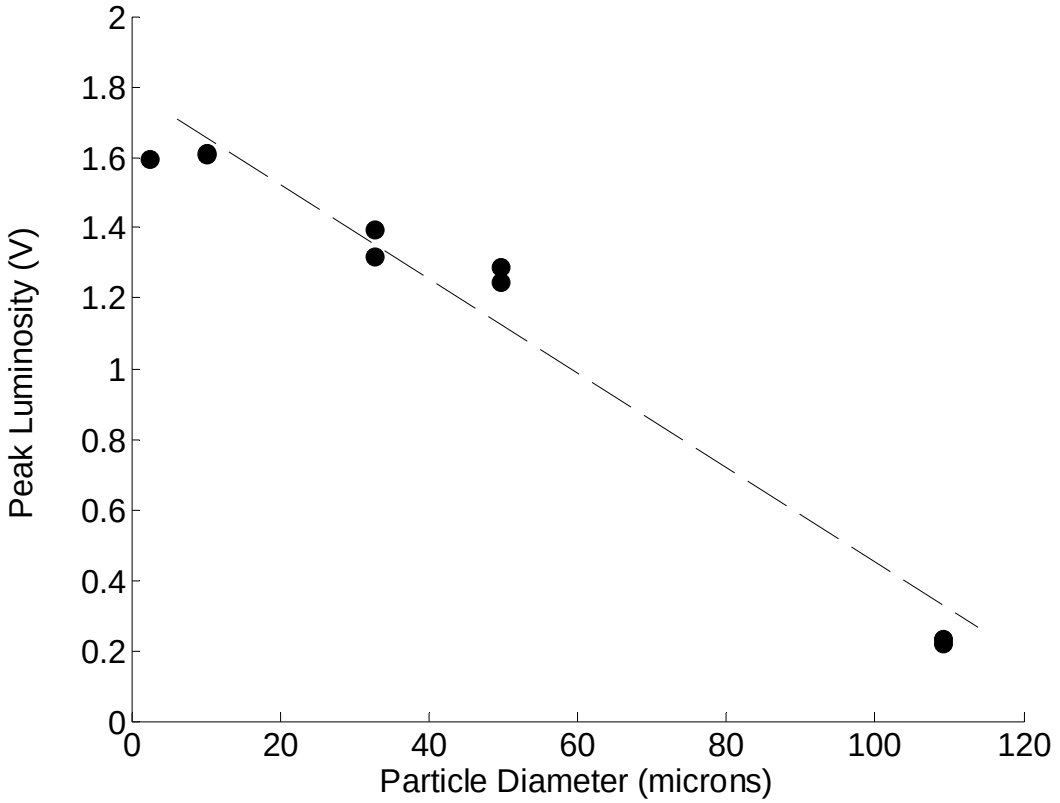

Figure 7. Luminosity amplitude as a function of particle size for all aluminum powders investigated.

time to be longer with a longer detonation tube.

Another possible explanation for the decreasing combustion time is that perhaps the particles do in fact burn to completion. It is possible that larger particles may burn to completion in a shorter time than smaller particles if the rate of consumption is higher. This may be the case since smaller particles come in mechanical equilibrium quicker than larger ones. This means that larger particles must be subjected to higher convective heat transfer rates as this is a strong function of the relative velocity between the particle and the flow.

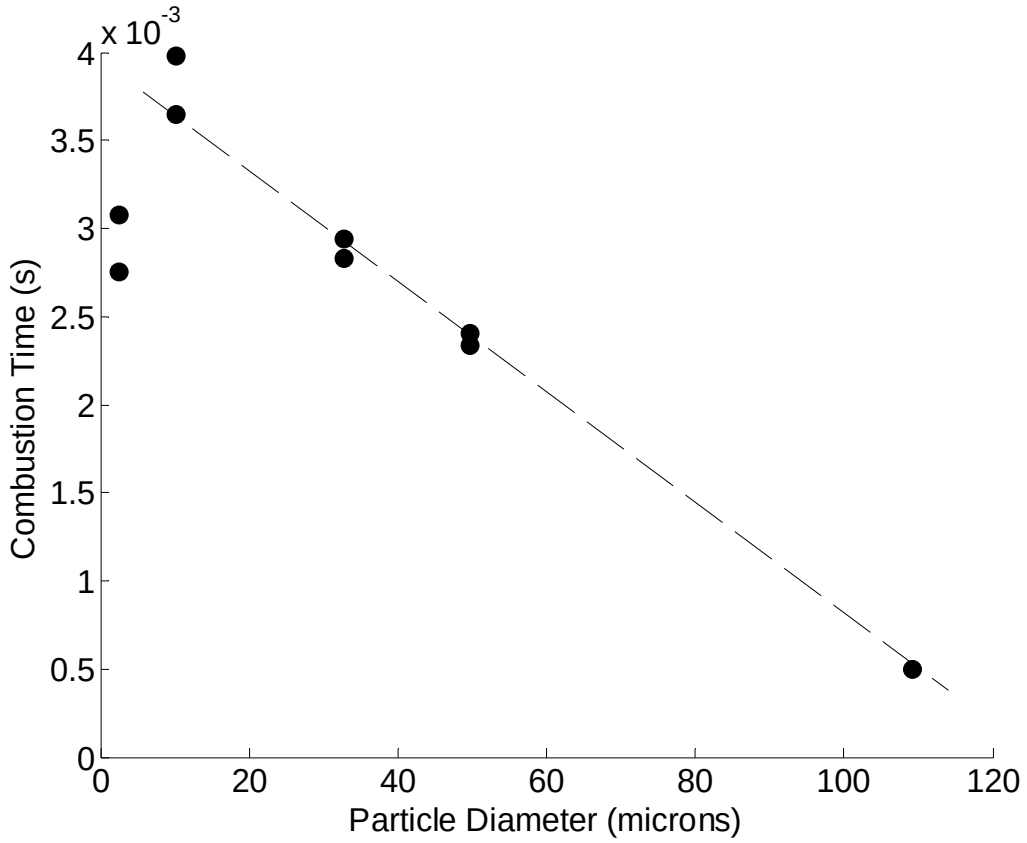

Figure 8. Combustion time (duration of the luminosity signal) as a function of particle size for all aluminum powders investigated.

Theoretical Considerations

Flow Field

The flow field in which the metal particles react is generated by a detonation wave propagating in a tube of stoichiometric hydrogen-oxygen. The detonation wave reaches a contact surface and transmits a shock wave into a tube of air. In order to predict the flow conditions the particles will encounter (such as flow velocity and temperature), one must be able to quantify the flow field.

The flow field generated by a detonation wave transmitting a shock wave in air is not analytically simple, particularly near the interface (where the metal particles are located). The solution of the non-reactive Euler equations was numerically obtained using a second order accurate slope-limiter centered scheme [6, 7]. The Taylor wave was solved analytically until the detonation reaches the interface. This was taken as the initial condition for the simulation.

Particle Trajectory

Neglecting body forces, the only force acting on a particle in the detonation products flow is a drag force. Newton's second law governs the particle motion:

$$F_D = \frac{1}{2} C_D A \rho v^2 = m_p a_p .$$

This equation can be rearranged and simplified to:

$$\frac{d^2x}{dt^2} = \frac{3}{4} \frac{C_D \rho(x,t)}{d_p \rho_p} \left| u(x,t) - \frac{dx}{dt} \right| \left[u(x,t) - \frac{dx}{dt} \right].$$

To integrate this equation, one requires the flow properties (velocity and density) and a drag coefficient, C_D, as well as particle properties. In this model, the correlation of Igra and Takayama [8] is used for the drag coefficient. This correlation, valid for Reynolds numbers ranging from 200 to 101,000, was obtained for unsteady particles in shock tubes and is given below:

$$\log C_D = a + b(\log Re) + c(\log Re)^2 + d(\log Re)^3 .$$

The empirical constants in this correlation are listed in Table 3.

Integrating the governing equation subject to the flow field solution obtained before, with

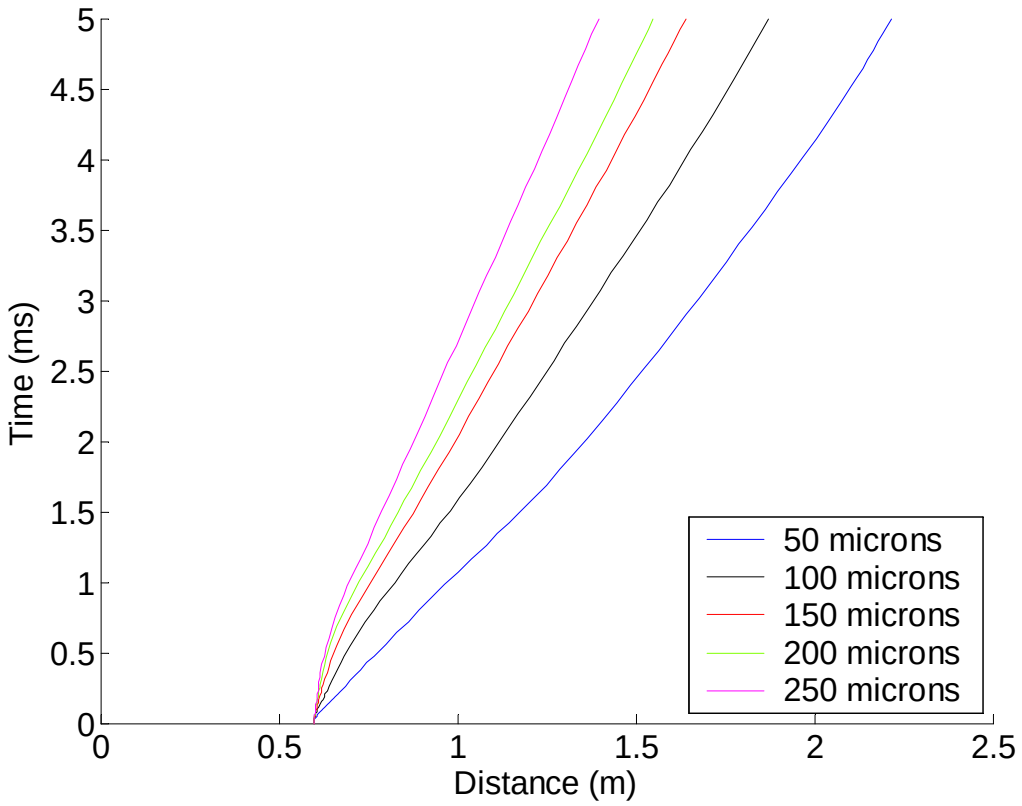

Figure 9. *x-t* diagram showing trajectories of 5 different magnesium particle sizes.

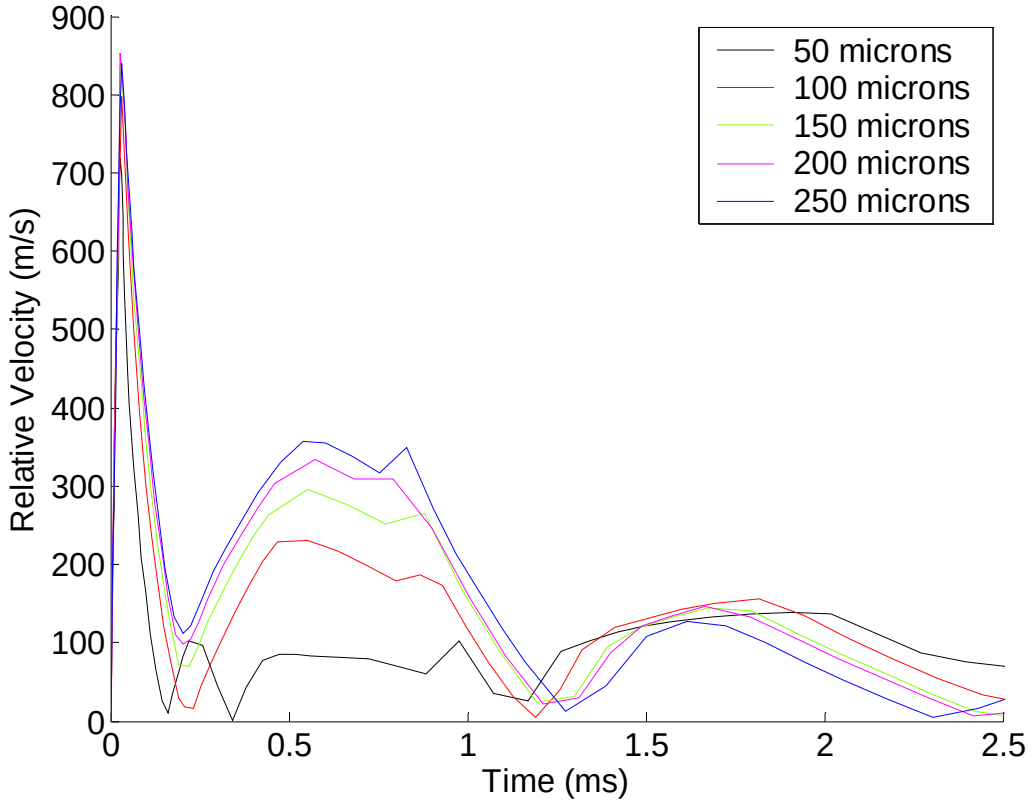

Figure 10. Absolute value of the relative velocity between the flow and magnesium particles of various sizes as a function of time.

given initial conditions (position and velocity) yields the trajectory of the particle. Figure 9 shows the trajectories of particles of different sizes on an *x*-*t* diagram.

Since convective heating is a strong function of the relative velocity between the gas and the particle, it is of interest to plot this relative velocity as a function of time for various particle sizes. This is shown in Fig. 10. As one would expect, initially, larger particles have a larger relative velocity (larger particles have more inertia and take a longer time to reach mechanical equilibrium with the flow). It is also interesting to note that the relative velocity drops quite sharply around 1 ms. Note as well that this drop occurs later for larger particles.

Particle Heating

In general, a particle is subject to convective and radiative heat transfer from (or to) the detonation products. Furthermore, heterogeneous surface reactions between the products and the particle also contribute to heating the particle.

In cases where the rate of convective heat transfer to the particle is much less than the rate of conductive heat transfer into the particle, a lumped capacitance analysis can be

used (temperature gradients can be neglected inside the particle). The criterion usually used is that the Biot number, $Bi < 0.1$, where

$$Bi \equiv \frac{h d_p}{k}.$$

A worst case scenario for the Biot number (largest Biot number) can be estimated for a given particle size by considering a particle immediately behind the detonation. At this point, the relative velocity of the particle as well as the temperature of the products (not yet expanded by the Taylor wave) would be a maximum, thereby maximizing the convective heat flux. In this study, the convective heat transfer coefficient, h, is obtained from Whitaker's [9] correlation for spheres:

$$Nu = 2 + (0.4\,\mathrm{Re}^{1/2} + 0.06\,\mathrm{Re}^{2/3})\,\mathrm{Pr}^{0.4}\left(\frac{\mu_\infty}{\mu_w}\right)^{0.25}.$$

The Nusselt number, Nu, in turn, is defined as:

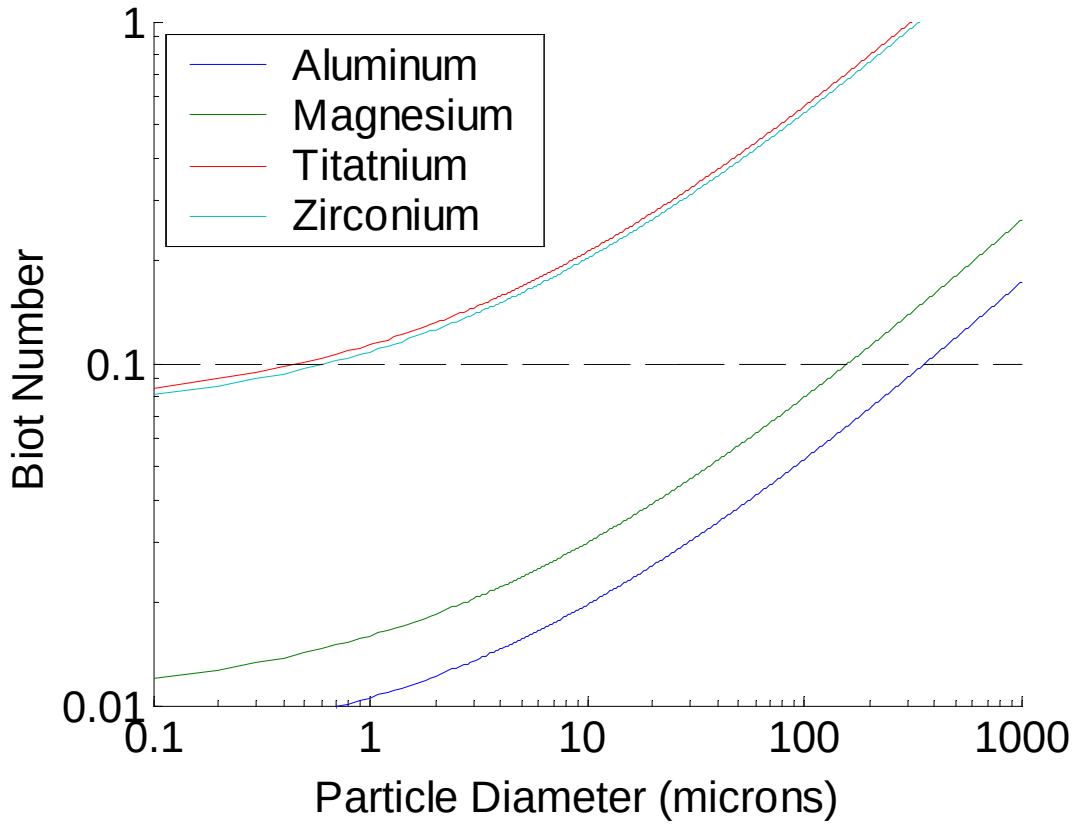

Figure 11. Biot number as a function of particle size for various metals. The Biot number is evaluated with the particle directly behind the detonation. This gives a worst case scenario.

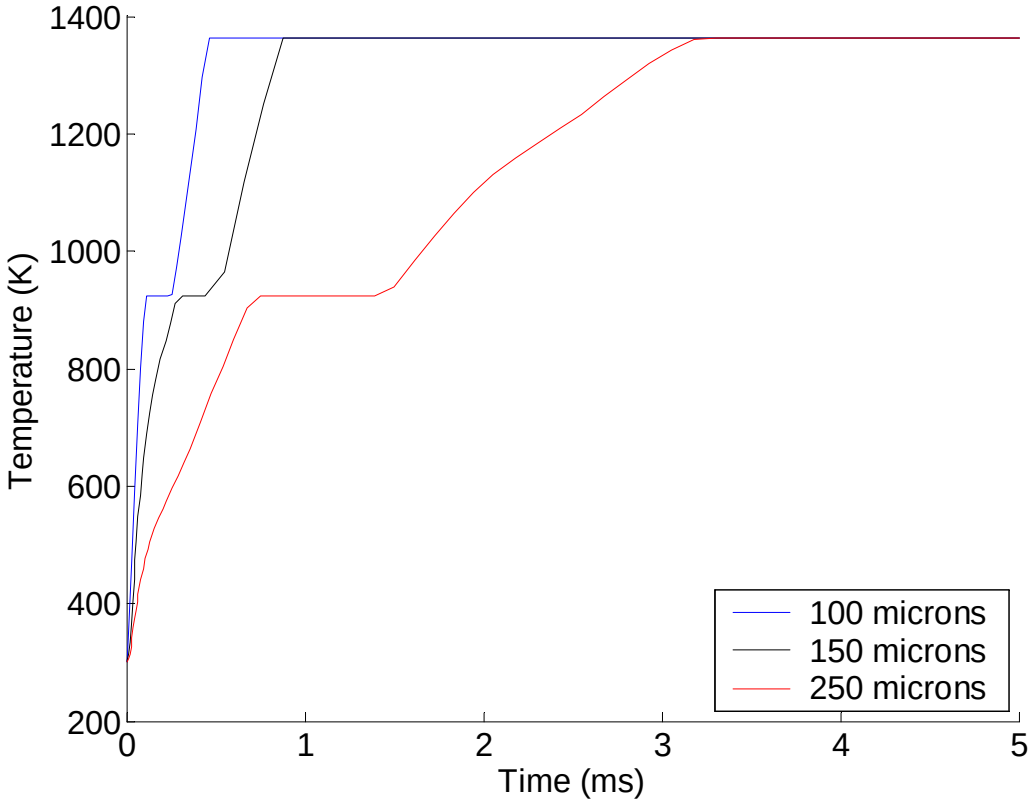

Figure 12. Temperature history of various sizes of magnesium particles.

$$Nu \equiv \frac{hd}{k_f}.$$

Figure 11 shows the value of the Biot number of aluminum, magnesium, titanium and zirconium particles immediately behind a hydrogen – oxygen detonation, as a function of particle size. Clearly, for aluminum and magnesium particles, a lumped capacitance analysis can be used for particles well above 100 μm. The largest particles used in this study are 240 μm magnesium particles. In this case, the Biot number is slightly more than 0.1, but considering that this is a worst case scenario (never experienced in the present study) the particles are considered to have a uniform temperature distribution. This fact tremendously simplifies the analysis. It should be noted that in the case of titanium and zirconium particles, the Biot number is less than 0.1 for particles less than 1 μm only. This is because their thermal conductivities are approximately one order of magnitude less than that of aluminum and magnesium. To treat these particles correctly, one would need to include temperature gradients (diffusion) inside the particles.

With the lumped capacitance analysis, the rearranged energy equation for a particle is:

$$\frac{dT_p}{dt} = \frac{6}{d_p \rho_p C_p}\left[h(T - T_p) + \varepsilon\sigma(T^4 - T_p^4) + \omega Q \right].$$

In this study, radiation and heterogeneous surface reactions are neglected. The melting of the particle is taken into account in the calculation. When the temperature of the particle reaches the melting point, the particle temperature is kept constant until an amount of heat equal to the latent heat of fusion is transferred to the particle.

Integrating the energy equation, subject to both the flow field and the particle trajectory obtained earlier, one obtains the temperature evolution of the particle. Figure 12 shows the temperature history of magnesium particles of various sizes. The first plateau at 923 K corresponds to the melting of the particles. The second plateau at 1363 K corresponds to the boiling point. Clearly larger particles take a longer time to heat up to the melting point and the boiling point.

Table 3. Constants in the drag coefficient correlation [8].

Constant	Value
a	7.8231
b	-5.8137
c	1.4129
d	-0.1146

Particle Reaction

For modeling purposes, the reaction of particle material is considered to occur as soon as the metal reaches the gas phase. For simplicity, it is assumed that this happens at a critical particle temperature. For metals such as magnesium, this temperature is usually taken as the metal boiling point, whereas for aluminum, the oxide melting point is usually used (Roberts et al. [3]). Integrating the above differential equations yields the particle trajectory and temperature. A comparison of the peak temperature reached by the particle and the "ignition temperature" reveals whether or not the particle was successfully ignited. The time at which the particle reaches the ignition temperature (if it ever does) is the reaction delay. Figure 12 clearly shows that the reaction delay (time to reach the boiling point of magnesium) increases with particle size. The reaction delay is plotted in Fig. 5 for both magnesium and aluminum as a function of particle size. Again, the reaction delay increases with particle size. This is expected as larger particles take a longer time to heat up to the critical temperature for ignition. These curves show good agreement for the small particles sizes (< 100 μm). Although both experiments and analytical results show an increase in delay time with particle size, the analytical curves increase more sharply such that at 240 μm, the model over predicts the data by a factor of 3 to 4. Nevertheless, the agreement is quite good and well within an order of magnitude. This suggests that the observed delay is indeed simply a result of particle heating.

Conclusions

Intense luminosity was observed for all the powders investigated. This luminosity was associated with chemical reaction. The light intensity was observed to decrease with increasing particle size. This is associated with the decreasing specific surface area of the larger particles. Although luminosity is observed quite rapidly in the experiment (after tens or hundreds of microseconds) the reaction time (as defined above) increases with increasing particle size. This trend is also obtained from analytical calculations including only convective heat transfer to the particle. The agreement of the experimental data and the analytical model is reasonable and suggests that the majority of the delay time observed is a result of convective heating of the particle to a critical temperature for chemical reaction. Finally, the duration of the chemical reaction was observed to decrease with increasing particle size.

Acknowledgements

The authors would like to acknowledge the dedicated assistance of Gary Ruddick in conducting the experiments as well as Eddie Ng for his CFD code and his precious assistance.

References

1. Frost, D.L., Zhang, F., Murray, S.B. and McCahan, S., "Critical Conditions for Ignition of Metal Particles in a Condensed Explosive," *Proceedings of 12th Detonation Symposium*, San Diego, California, 2002.

2. Frost, D.L. and Zhang, F., "Effect of Scale on the Blast Wave Generated by a Metallized Heterogeneous Explosive," *Energetic Materials: Reactions of Propellants, Explosives and Pyrotechnics*, Proc. 34th Int. Annual Conference of ICT, Karlsruhe, Germany, 7.1-7.14, 2003.

3. Roberts, TA, Burton, RL, Krier, H, "Ignition and Combustion of Aluminum/Magnesium Alloy Particles in O_2 at High Pressures," *Combustion and Flame*, Vol. 92 (1-2), pp. 125-143, 1993.

4. Fontijin, A., and Felder, W., "HTFFR Kinetics Studies of Al $+CO_2$ – AlO+CO, a non-Arrhenius Reaction," *J. Chem. Phys.*, Vol. 67(4), pp. 1561-1569, 1977.

5. Gordon, S., and McBride, B. J., Computer Code CEA, NASA, 1994.

6. Ng, H.D., The effect of chemical reaction kinetics on the structure of gaseous detonations, Ph.D. Thesis, McGill University, Canada, 2005.

7. Toro, E.F., *Riemann Solvers and Numerical Methods for Fluids Dynamics*, 2nd Edition, Springer-Verlag, Berlin, 1999.

8. Igra, O., and Takayama, K., "Shock Tube Study of the Drag Coefficient of a Sphere in a Non-Stationary Flow," *Proc. R. Soc. Lond. A*, 442:231-247, 1993.

9. Whitaker, S., "Forced Convection Heat-Transfer Correlations for Flow in Pipes, Past Flat Plates, Single Cylinders, Single Spheres, and Flow in Packed Beds and Tube Bundles," *AIChE J*., Vol. 18:361, 1972.